Structural and Multidisciplinary Optimization manuscript No.
(will be inserted by the editor)

Łukasz Jankowski

Off-line identification of dynamic loads

DOI 10.1007/s00158-008-0249-0
The original publication is available at http://www.springerlink.com/content/4755k35524031t17/
Received: 21 June 2007 / Revised: 22 January 2008 / Accepted: 6 February 2008 / Published online: 5 April 2008

Abstract This paper considers off-line identification of spatial and temporal characteristics of a dynamic load, and is focused on the case of a limited number of sensors. Both elastic and elasto-plastic structural behaviours are taken into account. The identification is performed off-line, based on optimisation of modelled local structural responses, and — in the case of limited number of sensors — identifies an observationally equivalent load, which in a given sense optimally approximates the actual load. Compared to previous researches this approach allows to identify general dynamic loads of unknown locations, including multiple impacts and moving loads, and gives more insight into the identification process by distinguishing between the reconstructible and unreconstructible load components. Additionally, the problem of optimum sensor location is discussed.

Keywords load identification · inverse dynamics · elasto-plastic structures · black box · forensic engineering

1 Introduction

This paper considers a methodology for a posteriori identification of spatial and temporal characteristics of dynamic loads. The motivation is the need for a general analysis technique for efficient reconstruction of the scenario of a sudden load (impact, collision etc.), to be applied in black-box type systems. The methodology is based on off-line analysis of local structural response (strain, acceleration etc.) and requires a dedicated sensors system to be distributed in the structure in order to measure and store the response. In the elasto-plastic case the Virtual Distortion Method (VDM) (Holnicki-Szulc and Gierliński 1995) is used, which is restricted to the small deformation case. The paper expands and builds upon the approach briefly outlined in Jankowski et al (2007).

There is an ongoing research effort in the field, see Chan et al (2001); Jacquelin et al (2003); Inoue et al (2001) for relatively recent reviews. However, the structures are assumed to be linear and the generality of the considered loads is usually strictly limited to a single pointwise load with the location known in advance (Wu et al 1998) or determined in an additional non-linear optimisation (Fukunaga and Hu 2006). Moreover, the identification is usually additionally simplified by assuming stationarity of the load. Law et al (1997); Chan et al (2001) do consider moving force, but it is assumed to have a constant velocity. A number of papers deals with single pointwise impact loads only and disregards all load characteristics (magnitude, evolution, duration etc.) besides the location (Gaul and Hurlebaus 1997; Martin and Doyle 1996). Papers that do consider multiple independent loads, as Adams and Doyle (2002), still assume superfluous number of sensors.

Compared to other researches, the approach discussed here is aimed at the fully general case. In the so-called *underestimated* case it allows to use a limited number of sensors to identify general dynamic loads of unknown locations, including simultaneous multiple impacts, freely moving and diffuse loads. However, this is at the cost of the uniqueness of identification, which can be attained only with additional heuristic assumptions. This way an equivalent load is identified, which is observationally indistinguishable from the actual load and optimum in a given sense. The identification is formulated analytically as a complex optimisation problem: find the equivalent impact scenario that

1. minimises the potentially pre-conditioned mean-square distance between simulated and measured dynamic responses in sensor locations and
2. is optimum according to given heuristic conditions.

The author gratefully acknowledges the financial support of the Polish Research Projects DIADYN (PBZ-KBN-105/T10/2003) and MATINT (PBZ-KBN-115/T08/2004). Parts of this paper will be used in a coming book „Smart Technologies for Safety Engineering" to be published by John Wiley & Sons in 2008.

Ł. Jankowski
Smart-Tech Centre, Institute of Fundamental Technological Research
Polish Academy of Sciences
Świetokrzyska 21, 00-049, Warsaw, Poland
E-mail: lukasz.jankowski@ippt.gov.pl

Since the identification accuracy is directly related to the number and location of sensors, two complementary criteria of correct sensor location are proposed, combined in a compound criterion and illustrated in a numerical example. Measurement noise, inevitable in real-world structures, is accounted for. In the case of elasto-plastic structures gradients of structural response are derived, which allow to apply any general gradient-based optimisation approach to identify the load.

2 Response to dynamic load

A prerequisite for the load identification methodology discussed here is the transfer function of the system being considered, i.e. the structural response to local impulse excitations and plastic distortions. It can be either generated from a numerical model or — at least partially — measured experimentally, the latter being potentially more practical in case of real-world complex structures.

2.1 Linear systems

Let the system being considered be linear and spatially discretised. Provided the system transfer function is known and no excitation prior to time $-\Delta T$ (i.e. zero initial conditions), the response of the system in a given sensor location can be expressed by means of a convolution integral as follows:

$$\varepsilon_\alpha(t) = \int_{-\Delta T}^{t} \mathbf{B}_\alpha^C(t-\tau)^T \mathbf{p}(\tau)\,\mathrm{d}\tau, \tag{1}$$

where ε_α is the response of the system in the α-th sensor location, vector $\mathbf{p}$ denotes the load evolution in all potentially load-exposed degrees of freedom (DOFs), while $\mathbf{B}_\alpha^C$ is the vector of the system transfer functions $B_{\alpha n}^C$ relating the response in the α-th sensor location to local impulse load in the n-th potentially load-exposed DOF.

ΔT is in (1) the maximum system response time (i.e. the maximum propagation time of an elastic wave between a load-exposed DOF and a sensor). Due to the intended limited number of sensors the considered system is rarely collocated, thus $\Delta T > 0$. The measurements and the identification process may be triggered by a strong excitation (e.g. an impact), which is picked up delayed at most ΔT, hence the time shift is necessary.

In real-world applications only discretised responses are known, hence (1) should be discretised with respect to time. With the simplest quadrature rule it takes the following form

$$\varepsilon_\alpha(t) = \sum_{\tau=-\Delta T}^{t} \mathbf{B}_\alpha(t-\tau)^T \mathbf{p}(\tau), \tag{2}$$

where $\mathbf{B}_\alpha$ is the discretised and accordingly rescaled system transfer function $\mathbf{B}_\alpha = \Delta t \mathbf{B}_\alpha^C$. Equation 2, rewritten for each sensor location α and each measurement time instance t, can be stated in the form of a general linear equation:

$$\varepsilon = \mathbf{B}\mathbf{p} \tag{3}$$

where ε is the vector of system responses in all sensor locations α and *measurement* time instances $t = 0, \dots T$, load vector $\mathbf{p}$ represents the loading forces in all load-exposed degrees of freedom and in all *loading* time instances $\tau = -\Delta T, \dots T$, while $\mathbf{B}$ is the system transfer matrix compound of discretised $\mathbf{B}_\alpha$.

2.2 Elasto-plastic systems

The stated above description of system dynamics can be extended to include the elasto-plastic system behaviour by combining the computationally effective Virtual Distortion Method (VDM) (Holnicki-Szulc and Gierliński 1995) with the return-mapping algorithm (Simo and Hughes 1989), see also Wikło and Holnicki-Szulc (2008). The small deformation restriction still applies and the extension is obviously at the cost of the linearity. For notational simplicity only trusses are considered here and $\varepsilon_\alpha(t)$ denotes in this subsection the strain in the α-th truss element, although with inessential modifications the concept is applicable to other types of structures and linear sensors (for frames and plates see Putresza and Kołakowski (2001) or Holnicki-Szulc and Gierliński (1995)). Trusses are however conceptually the simplest to describe, since each element is associated with only one (axial) plastic distortion state, while already three states are necessary for a frame element (axial, pure bending and bending/shear) and even more for other elements. Nevertheless, the governing equations remain basically the same, although non-truss structures require more variables and are hence notationally and computationally more demanding.

In the elasto-plastic case (2) has to take into account the effect of the plastic distortions of the truss elements,

$$\varepsilon_\alpha(t) = \sum_{\tau=-\Delta T}^{t} \mathbf{B}_\alpha(t-\tau)^T \mathbf{p}(\tau) + \sum_{\tau=-\Delta T}^{t} \mathbf{B}_\alpha^P(t-\tau)^T \beta(\tau), \tag{4}$$

where vector β contains the discretised plastic distortions of all truss elements and $\mathbf{B}_\alpha^P$ is the vector of the discrete system transfer functions $B_{\alpha\zeta}^P$ relating the response in the α-th sensor location (i.e. the strain in the α-th element according to the convention of this subsection) to the unit plastic distortion of the ζ-th truss element. According to VDM, plastic distortion is to be identified with plastic strain and is modelled by a pair of self-equilibrated forces, which are applied at the nodes of the concerned element so that in the static case it would be respectively (elastically) strained. In the dynamic case the distortions and the forces are time-dependent. (4), as very similar to (1), seems to be linear, but it obviously cannot be the case here. One of the reasons is the plastic distortion β being non-linearly dependent on the load $\mathbf{p}$.

Only isotropic hardening plasticity is considered in the following as a relatively basic example requiring only one internal hardening variable $\Psi_\alpha(t)$, which denotes the *total plastic strain*:

$$\begin{aligned} \Psi_\alpha(t+\Delta t) &= \Psi_\alpha(t) + |\Delta\beta_\alpha(t+\Delta t)|, \\ \Delta\beta_\alpha(t+\Delta t) &= \beta_\alpha(t+\Delta t) - \beta_\alpha(t). \end{aligned} \tag{5}$$

The yield criterion can be expressed in the case of isotropic hardening via the total plastic strain as follows:

$$|\sigma_\alpha(t+\Delta t)| = \sigma_\alpha^* + \frac{\gamma_\alpha}{1-\gamma_\alpha} E_\alpha \Psi_\alpha(t+\Delta t), \tag{6}$$

where σ_α^*, γ_α and E_α are respectively the initial plastic flow stress, the hardening coefficient and Young's modulus of the α-th truss element. Other plasticity models can be relatively easy obtained by increasing the number of internal variables, see Simo and Hughes (1989).

To determine the set of elements yielding in each time step and the actual amounts of plastic flows, the *trial strain* $\varepsilon_\alpha^{\mathrm{tr}}(t+\Delta t)$ and the *trial stress* $\sigma_\alpha^{\mathrm{tr}}(t+\Delta t)$ have to be computed by *freezing the plastic flow* and performing a purely elastic step, which amounts to a temporary assumption $\beta(t+\Delta t) := \beta(t)$ in (4):

$$\begin{aligned} \varepsilon_\alpha^{\mathrm{tr}}(t+\Delta t) &= \varepsilon_\alpha(t+\Delta t) - \mathbf{B}_\alpha^P(0)^T \Delta\beta(t+\Delta t), \\ \sigma_\alpha^{\mathrm{tr}}(t+\Delta t) &= E_\alpha\left[\varepsilon_\alpha^{\mathrm{tr}}(t+\Delta t) - \beta_\alpha(t)\right]. \end{aligned} \tag{7}$$

The actual stress $\sigma_\alpha(t+\Delta t)$ in the α-th element at time $t+\Delta t$ can be expressed in two ways:

1. In terms of Young's modulus and the actual values of the strain and the plastic distortion as

   $$\sigma_\alpha(t+\Delta t) = E_\alpha\left[\varepsilon_\alpha(t+\Delta t) - \beta_\alpha(t+\Delta t)\right],$$

   which by (5) and (7) can be transformed to

   $$\begin{aligned} &\sigma_\alpha(t+\Delta t) \\ &= E_\alpha\left[\varepsilon_\alpha^{\mathrm{tr}}(t+\Delta t) + \mathbf{B}_\alpha^P(0)^T \Delta\beta(t+\Delta t)\right] \\ &\quad - E_\alpha\left[\beta_\alpha(t) + \Delta\beta_\alpha(t+\Delta t)\right] \\ &= \sigma_\alpha^{\mathrm{tr}}(t+\Delta t) + E_\alpha \sum_\zeta \left[B_{\alpha\zeta}^P(0) - \delta_{\alpha\zeta}\right] \Delta\beta_\zeta(t+\Delta t), \end{aligned} \tag{8}$$

   where $\delta_{\alpha\zeta}$ is Kronecker's delta.
2. Provided the element is yielding, the stress $\sigma_\alpha(t+\Delta t)$ can be also obtained by multiplying the yield criterion (6) by $\operatorname{sgn}\sigma_\alpha(t+\Delta t)$ and noticing that for isotropic hardening the trial stress $\sigma_\alpha^{\mathrm{tr}}$, the actual stress σ_α and the plastic flow $\Delta\beta_\alpha$ are in each time step all of the same sign,

   $$\begin{aligned} \sigma_\alpha(t+\Delta t) &= \sigma_\alpha^* \operatorname{sgn}\sigma_\alpha^{\mathrm{tr}}(t+\Delta t) \\ &\quad + \frac{\gamma_\alpha}{1-\gamma_\alpha} E_\alpha\left[\Psi_\alpha(t) \operatorname{sgn}\sigma_\alpha^{\mathrm{tr}}(t+\Delta t) + \Delta\beta_\alpha(t+\Delta t)\right]. \end{aligned} \tag{9}$$

Equations 8 and 9 combined together yield the following linear set of equations for the plastic flow $\Delta\beta_\alpha(t+\Delta t)$:

$$\begin{aligned} &E_\alpha \sum_{\zeta\in Y_{t+\Delta t}} \left[B_{\alpha\zeta}^P(0) - \frac{\delta_{\alpha\zeta}}{1-\gamma_\alpha}\right] \Delta\beta_\zeta(t+\Delta t) = -\sigma_\alpha^{\mathrm{tr}}(t+\Delta t) \\ &+ \left[\sigma_\alpha^* + \frac{\gamma_\alpha}{1-\gamma_\alpha} E_\alpha \Psi_\alpha(t)\right] \operatorname{sgn}\sigma_\alpha^{\mathrm{tr}}(t+\Delta t), \end{aligned} \tag{10}$$

which are valid only for the elements, which are actually yielding $\{\alpha,\zeta\} \in Y_{t+\Delta t}$. The set $Y_{t+\Delta t}$ has to be found iteratively by applying the yield criterion (6) to the trial stresses $\sigma_\alpha^{\mathrm{tr}}(t+\Delta t)$ and, if necessary, to the stresses computed consecutively by (10) and (7).

3 Load identification

Load identification amounts basically to a deconvolution: compare the measured ε^M and the modelled ε system responses, and obtain the excitation by solving the resulting system of equations. For a linear system it leads to either a system of several Volterra integral equations of the first kind (the continuous time case), see (1),

$$\varepsilon_\alpha^M(t) = \int_{-\Delta T}^{t} \mathbf{B}_\alpha^C(t-\tau)^T \mathbf{p}(\tau), \tag{11}$$

or, in the discrete time case, to a large system of linear equations, see (3),

$$\varepsilon^M = \mathbf{B}\mathbf{p}. \tag{12}$$

An elasto-plastic system, see (4), yields the following set of non-linear equations

$$\varepsilon_\alpha^M(t) = \sum_{\tau=-\Delta T}^{t} \mathbf{B}_\alpha(t-\tau)^T \mathbf{p}(\tau) + \sum_{\tau=-\Delta T}^{t} \mathbf{B}_\alpha^P(t-\tau)^T \beta(\tau). \tag{13}$$

In all cases the unknown is the load vector $\mathbf{p}$.

Equation 12 is a large linear system, with the vectors ε^M and $\mathbf{p}$ containing respectively the measured discretised system response and the discretised loading forces, while $\mathbf{B}$ is the system transfer matrix. By a proper reordering of the vectors ε^M and $\mathbf{p}$, the matrix $\mathbf{B}$ can take the rearranged form of a large block matrix composed of Toeplitz matrices relating discretised sensor responses to unit excitations in all potentially load-exposed DOFs, see an example in Figure 6.

Note that in the intended practical situations the linear system (12) is usually underdetermined, i.e. there are significantly fewer equations than unknowns being sought. The reason is twofold: (i) there are significantly fewer sensors than potentially load-exposed DOFs; (ii) time intervals of different length (measurement T and reconstruction $T+\Delta T$) are discretised with the same time step Δt. More precisely, let A be the number of sensors, N the number of potentially load-exposed DOFs, T the length of the reconstruction time interval and Δt the time discretisation. Then in the linear system (12) there are $AT/\Delta t$ equations (related to the measurements) and $N(T+\Delta T)/\Delta t$ unknowns (related to the load being identified). Moreover, even with sufficiently many sensors and equations, a specific topology of the mechanical system being modelled can decrease the rank of the matrix $\mathbf{B}$ and make it underdetermined.

Both the continuous (11) and the discrete (12) tend to be ill-conditioned. This is mainly due to the inherent ill-conditioning of compact integral operators of the first kind, which cannot have a bounded inverse (Kress 1989). A seemingly contradictory behaviour is the result: the finer the time discretisation Δt, the more ill-conditioned (12) is. Moreover, the ill-conditioning of (12) may arise also due to system non-collocation and small or neglected time shift ΔT, which results in the block matrix $\mathbf{B}$ including almost triangular Toeplitz matrices with very small values near the diagonal. Therefore, a regularisation technique is usually a must

(Jacquelin et al 2003; Kress 1989; Hansen 2002; Tikhonov and Arsenin 1977).

Note also that the linear system (12) can be easily preconditioned by substituting $\varepsilon^M \leftarrow \mathbf{M}\varepsilon^M$ and $\mathbf{B} \leftarrow \mathbf{MB}$ to take effectively the form $\mathbf{M}\varepsilon^M = \mathbf{MBp}$, provided the matrix $\mathbf{M}$ is of appropriate dimensions. Preconditioning may be desired in order to weight the response of different sensors or to speed up the optimisation-based identification process (Nocedal and Wright 1999). For reasons of notational simplicity no preconditioning (or an identity preconditioner matrix $\mathbf{M} = \mathbf{I}$) is assumed further on.

Real-world measurements are always discrete, hence the continuous time case is dropped from the following as impractical. The next two parts deal with the over- and underdetermined discrete linear cases, while the third part considers the elasto-plastic case.

3.1 Overdetermined linear systems

If the system (12) is overdetermined, a unique generalised load can be found to minimise its residuum. The direct way to find it would be to use the pseudoinverse $\mathbf{B}^+$, which can be obtained e.g. via the singular value decomposition (SVD) of the matrix $\mathbf{B}$. Moreover, the use of SVD would allow direct truncating too small singular values, which is a common regularisation technique. However, as matrix $\mathbf{B}$ is usually very large, a quicker and less memory-consuming way may be to use iterative methods to minimise the residuum of (12), possibly coupled with the Tikhonov regularisation term (Hansen 2002; Tikhonov and Arsenin 1977; Jacquelin et al 2003).

3.1.1 Objective function

The system (12) can be solved via the least-squares approach (Dahlquist and Bjørck 2006) using the following objective function:

$$f(\mathbf{p}) = \left\|\varepsilon^M - \mathbf{Bp}\right\|^2 + \delta \left\|\mathbf{Dp}\right\|^2, \tag{14}$$

where $\|\mathbf{Dp}\|^2$ is a Tikhonov regularisation term and $\delta \geq 0$ may be assigned a specific numerical value e.g. by means of the L-curve technique (Kress 1989; Hansen 2002; Tikhonov and Arsenin 1977; Jacquelin et al 2003). Taking into account (2) and (3), the objective function can be thus rewritten as

$$f(\mathbf{p}) = \sum_{\alpha} \sum_{t=0}^{T} \left[\varepsilon_\alpha^M(t) - \varepsilon_\alpha(t)\right]^2 + \delta \left\|\mathbf{Dp}\right\|^2, \tag{15}$$

while its derivatives can be expressed as

$$\begin{aligned} \frac{\partial f(\mathbf{p})}{\partial p_n(t)} &= \delta \frac{\partial \left\|\mathbf{Dp}\right\|^2}{\partial p_n(t)} \\ &\quad - 2 \sum_{\alpha} \sum_{\substack{\tau= \\ max(0,t)}}^{T} \left[\varepsilon_\alpha^M(\tau) - \varepsilon_\alpha(\tau)\right] B_{\alpha n}(\tau - t), \end{aligned} \tag{16}$$

where $p_n(t)$ and $B_{\alpha n}$ are respectively elements of the vectors $\mathbf{p}(t)$ and $\mathbf{B}_\alpha$, and

$$\frac{\partial \left\|\mathbf{Dp}\right\|^2}{\partial p_i} = 2\left[\mathbf{D}^T\mathbf{Dp}\right]_i. \tag{17}$$

Note that the formulae (15) and (16), as well as (19) below, make use of the special form of the system matrix $\mathbf{B}$ in order to spare the numerical costs by one order of magnitude. However, they hold for the assumed identity preconditioner matrix $\mathbf{M} = \mathbf{I}$ only, and in other cases have to be replaced by their general counterparts.

The objective function (14) is convex and quadratic, thus it can be exactly expanded around a given load vector $\mathbf{p}$ as

$$f(\mathbf{p}+\mathbf{d}) = f(\mathbf{p}) + \nabla f(\mathbf{p})^T\mathbf{d} + \frac{1}{2}\mathbf{d}^T\mathbf{Hd}, \tag{18}$$

where $\mathbf{H} = \nabla^2 f$ is the positive semidefinite Hessian of f. Equation 18 compared with (15) yields the two following basic formulae:

$$\begin{aligned} \nabla f(\mathbf{p})^T\mathbf{d} &= 2\delta\mathbf{p}^T\mathbf{D}^T\mathbf{Dd} \\ &\quad - 2\textstyle\sum_\alpha \sum_{t=0}^{T} \varepsilon_\alpha^{(\mathbf{d})} \left[\varepsilon_\alpha^M(t) - \varepsilon_\alpha^{(\mathbf{p})}(t)\right], \\ \mathbf{d}_i^T\mathbf{Hd}_j &= 2\delta\mathbf{d}_i^T\mathbf{D}^T\mathbf{Dd}_j + 2\textstyle\sum_\alpha \sum_{t=0}^{T} \varepsilon_\alpha^{(\mathbf{d}_i)}(t)\, \varepsilon_\alpha^{(\mathbf{d}_j)}(t), \end{aligned} \tag{19}$$

where $\varepsilon_\alpha^{(\mathbf{d})}$ denotes the response in the α-th sensor location to the excitation $\mathbf{d}$.

3.1.2 Line optimisation

The iterative optimisation method used here consist of a series of line optimisations. Each one amounts to finding the minimum of f at a given load $\mathbf{p}$ along a given direction $\mathbf{d}$, i.e. the minimum of $f(\mathbf{p}+s\mathbf{d})$ with respect to s. Due to (18) this is a convex quadratic function with the minimum

$$s_{min} = -\frac{\nabla f(\mathbf{p})^T\mathbf{d}}{\mathbf{d}^T\mathbf{Hd}}, \tag{20}$$

which is directly calculable by (19).

3.1.3 Conjugate gradient

Given a load $\mathbf{p}$, the minimum along each optimisation direction $\mathbf{d}$ can be directly calculated by (20). However, first the optimisation direction $\mathbf{d}$ has to be chosen.

Equations 16 and 17 allow to calculate directly the steepest descent direction $-\nabla f(\mathbf{p})$. The objective function is unbounded quadratic, thus perfectly suited for the conjugate gradient method: choosing in the $(n+1)$-th optimisation step the direction $\mathbf{d}_{n+1}$ *conjugate* to all previous optimisation directions $\mathbf{d}_0, \ldots, \mathbf{d}_n$ yields by (20) directly the minimum in the subspace spanned by all considered directions $\mathrm{span}(\mathbf{d}_0, \ldots, \mathbf{d}_n)$.

Table 1 Optimisation algorithm for the overdetermined case

Initial calculations:	
1) initialise	$\mathbf{p}_0 := \mathbf{0}, \quad \varepsilon^{(\mathbf{p}_0)} := \mathbf{0}, \quad n := 0$
The loop:	
2) calculate	$\mathbf{d}_n := -\nabla f(\mathbf{p}_n), \quad \varepsilon^{(\mathbf{d}_n)}$
3) conj. direction	for$(i = 0; i < n, ++i)$
(3a)	$\eta := -\mathbf{d}_n^T \mathbf{H} \mathbf{d}_i$
(3b)	$\mathbf{d}_n := \mathbf{p}_n + \eta\, \mathbf{d}_i$
(3c)	$\varepsilon^{(\mathbf{d}_n)} := \varepsilon^{(\mathbf{d}_n)} + \eta\, \varepsilon^{(\mathbf{d}_i)}$
4) normalise (4a)	$D := \sqrt{\mathbf{d}_n^T \mathbf{H} \mathbf{d}_n}$
(4b)	$\mathbf{d}_n := \mathbf{d}_n / D$
(4c)	$\varepsilon^{(\mathbf{d}_n)} := \varepsilon^{(\mathbf{d}_n)} / D$
5) line minimum	$s := -\nabla f(\mathbf{p}_n)^T \mathbf{d}_n$
6) store	$\mathbf{d}_n, \quad \varepsilon^{(\mathbf{d}_n)}$
7) update (7a)	$\mathbf{p}_{n+1} := \mathbf{p}_n + s\, \mathbf{d}_n$
(7b)	$\varepsilon^{(\mathbf{p}_{n+1})} := \varepsilon^{(\mathbf{p}_n)} + s\, \varepsilon^{(\mathbf{d}_n)}$
(7c)	$n := n + 1$

Therefore, starting with the steepest descent direction and making use of the conjugacy criterion $\mathbf{d}_i^T \mathbf{H} \mathbf{d}_j = 0$,

$$\mathbf{d}_{n+1} = -\nabla f(\mathbf{p}_{n+1}) + \sum_{i=0}^{n} \eta_{n+1,i} \mathbf{d}_i, \tag{21}$$

where

$$\eta_{n+1,i} = \frac{\nabla f(\mathbf{p}_{n+1})^T \mathbf{H} \mathbf{d}_i}{\mathbf{d}_i^T \mathbf{H} \mathbf{d}_i},$$

which is basically Gram-Schmidt orthogonalisation scheme. The calculations start with the steepest descent direction, hence in exact arithmetic $\eta_{n+1,i} = 0$ for $i = 0, 1, \ldots, n-1$, which is a useful property of the conjugate gradient method, see e.g. Nocedal and Wright (1999). However, the limited accuracy of the floating point arithmetic makes all the correction terms necessary.

3.1.4 The algorithm

The algorithm for the overdetermined case is presented in Table 1. The most expensive operations are the calculations of the gradient and of the corresponding response (step 2). Moreover, at large step numbers n, it is quicker to calculate the response $\varepsilon^{(\mathbf{d}_n)}$ directly by (2) than to superpose the stored responses (step 3c).

3.2 Underdetermined linear systems

All known research, see e.g. Inoue et al (2001); Chan et al (2001); Jacquelin et al (2003) for reviews and analysis, deals with the overdetermined case only. However, in real-world applications the number of sensors is limited by practical reasons. Therefore, in the overdetermined case the generality of the load being identified must be significantly limited. As mentioned in the introduction, the load has been usually assumed to be a single stationary (or moving at a constant velocity) pointwise force, while its location is assumed to be known in advance or determined by a second-stage nonlinear optimisation: freely moving, diffuse or multiple loads are excluded. The approach proposed in this subsection addresses the general underdetermined case directly, although at the cost of the identification uniqueness. This allows to take into account all general loading patterns.

Generally, with an underdetermined system (12), the unknown load $\mathbf{p}$ can be identified in two ways, which differ in accuracy and numerical costs per single identification (time, memory etc.). The information lost in measurement in an underdetermined system can be completed by heuristic assumptions only, hence they play an important role in both methods.

- The more accurate approach requires singular value decomposition (SVD) of the matrix $\mathbf{B}$, which is numerically costly, but one-time only. Thereupon, given a measured response vector ε^M, two complementary components of the corresponding load can be relatively quickly identified: the reconstructible component (based on the measurements ε^M) and the unreconstructible component (based on the heuristic assumptions).
- The less accurate approach makes no distinction between both load components and identifies them simultaneously. The system (12) is first transformed to a larger overdetermined system using heuristic (and in fact regularising) assumptions and then solved using the iterative approach presented above for overdetermined systems. The numerically costly singular value decomposition of the obtained augmented system is hence not required, but at the expense of higher numerical cost per single identification. This approach is generally less accurate, since the heuristic assumptions influence both reconstructible and unreconstructible components of the load being identified, while the former component can — and thus should — be identified on the basis of the measurements ε^M only. The solution of the augmented system by SVD is possible, but prohibitive in terms of the numerical costs due to its size.

3.2.1 Load decomposition

The matrix $\mathbf{B}$ of (12) has a singular value decomposition (SVD),

$$\mathbf{B} = \mathbf{U} \Sigma \mathbf{V}^T, \tag{22}$$

where $\mathbf{U}$, $\mathbf{V}$ are square unitary matrices, i.e. $\mathbf{U}^T \mathbf{U} = \mathbf{U}\mathbf{U}^T = \mathbf{I}$, $\mathbf{V}^T \mathbf{V} = \mathbf{V}\mathbf{V}^T = \mathbf{I}$. Their dimensions equal respectively the number of equations and the number of unknowns. The matrix Σ is a rectangular diagonal matrix of appropriate dimensions, its diagonal values are called singular values of $\mathbf{B}$ and are customary ordered non-increasing. The SVD decomposition (22) is unique up to the permutation of the singular values (Dahlquist and Bjørck 2006).

The system (12) is usually very ill-conditioned, which is indicated by its singular values (diagonal elements of Σ)

spanning across several orders of magnitude. A regularisation is then a must, which — given the SVD (22) — may be performed straightforward by zeroing too small singular values, i.e. the values below the threshold level defined by the expected relative measurement accuracy $\varepsilon \geq 0$, see Jacquelin et al (2003); Hansen (2002); Tikhonov and Arsenin (1977). This way modified diagonal and system matrices Σ^ε, $\mathbf{B}^\varepsilon$ are obtained and (22) takes the following regularised form

$$\mathbf{B}^\varepsilon = \mathbf{U}\Sigma^\varepsilon\mathbf{V}^T. \tag{23}$$

Note that at $\varepsilon = 0$ all singular values are preserved: $\mathbf{B}^0 = \mathbf{B}$.

Let $\mathbf{P}$ be the linear space of all possible loads $\mathbf{p}$. Let $\mathbf{V}_1^\varepsilon$ and $\mathbf{V}_2^\varepsilon$ denote the two matrices composing together the matrix $\mathbf{V} = [\mathbf{V}_1^\varepsilon\,\mathbf{V}_2^\varepsilon]$, where the number of columns of $\mathbf{V}_1^\varepsilon$ equals the number of positive singular values of $\mathbf{B}^\varepsilon$, i.e. the number of positive diagonal values of Σ^ε. The matrix $\mathbf{V}$ is unitary, thus the columns of $\mathbf{V}_1^\varepsilon$ and $\mathbf{V}_2^\varepsilon$ are mutually orthonormal vectors, constitute an orthonormal basis in $\mathbf{P}$ and hence span two orthogonal and complementary linear subspaces $\mathbf{P}_1^\varepsilon$ and $\mathbf{P}_2^\varepsilon$:

$$\mathbf{P} = \mathbf{P}_1^\varepsilon \times \mathbf{P}_2^\varepsilon, \quad \mathbf{P}_1^\varepsilon = \operatorname{span}\mathbf{V}_1^\varepsilon, \quad \mathbf{P}_2^\varepsilon = \operatorname{span}\mathbf{V}_2^\varepsilon. \tag{24}$$

Due to (23) $\mathbf{P}_2^\varepsilon = \ker\mathbf{B}^\varepsilon$, i.e.

$$\mathbf{B}^\varepsilon\mathbf{V}_2^\varepsilon = \mathbf{0}, \tag{25}$$

and hence the regularised system transfer matrix $\mathbf{B}^\varepsilon$ is a linear measurement operator, which effectively: (i) transforms $\mathbf{P}$ orthonormally, (ii) projects it onto $\mathbf{P}_1^\varepsilon$, losing a part of the load information, (iii) rescales along the basis directions by Σ^ε, and finally (iv) transforms again orthonormally via $\mathbf{U}$. Therefore, with respect to $\mathbf{B}^\varepsilon$, $\mathbf{P}_1^\varepsilon$ is the reconstructible subspace and $\mathbf{P}_2^\varepsilon$ is the unreconstructible subspace of $\mathbf{P}$. In other words, given the relative measurement accuracy $\varepsilon \geq 0$, *each load* $\mathbf{p}$ *can be uniquely decomposed into a sum of two orthogonal components*,

$$\begin{aligned}\mathbf{p} = \mathbf{V}\mathbf{V}^T\mathbf{p} &= \mathbf{V}_1^\varepsilon\mathbf{V}_1^{\varepsilon T}\mathbf{p} + \mathbf{V}_2^\varepsilon\mathbf{V}_2^{\varepsilon T}\mathbf{p} \\ &= \mathbf{V}_1^\varepsilon\mathbf{m}_1 + \mathbf{V}_2^\varepsilon\mathbf{m}_2 = \mathbf{p}_R^\varepsilon + \mathbf{V}_2^\varepsilon\mathbf{m}_2,\end{aligned} \tag{26}$$

where

1. the first component $\mathbf{p}_R^\varepsilon = \mathbf{V}_1^\varepsilon\mathbf{V}_1^{\varepsilon T}\mathbf{p} = \mathbf{V}_1^\varepsilon\mathbf{m}_1$ is a linear combination of columns of $\mathbf{V}_1^\varepsilon$, and hence fully reconstructible from the noisy measurements $\varepsilon^M = \mathbf{B}\mathbf{p}$, while
2. the second component $\mathbf{V}_2^\varepsilon\mathbf{m}_2$ is a linear combination of columns of $\mathbf{V}_2^\varepsilon$, and hence unreconstructible, since all respective information is lost due to (25) in the noisy measurement process represented by the linear operator $\mathbf{B}^\varepsilon$ (because $\mathbf{B}^\varepsilon\mathbf{V}_2^\varepsilon\mathbf{m}_2 = \mathbf{0}$) and is hence not retained above the required relative degree of accuracy $\varepsilon \geq 0$ in the noisy measurements $\mathbf{B}^\varepsilon\mathbf{p}$.

3.2.2 Reconstructible load component

Given the noisy measurements ε^M and the regularised system matrix $\mathbf{B}^\varepsilon$, the unique reconstructible load component $\mathbf{p}_R^\varepsilon = \mathbf{V}_1^\varepsilon\mathbf{m}_1^\varepsilon$ can be found either

- directly by the standard pseudoinverse $\mathbf{B}^{\varepsilon+}$ of the regularised system matrix $\mathbf{B}^\varepsilon$,

$$\mathbf{p}_R^\varepsilon = \mathbf{B}^{\varepsilon+}\varepsilon^M = \mathbf{V}\Sigma^{\varepsilon+}\mathbf{U}^T\varepsilon^M, \tag{27}$$

  where the diagonal matrix $\Sigma^{\varepsilon+}$ is obtained from Σ^ε by transposition and replacement of all non-zero elements by their reciprocals, or
- by solving the system $\varepsilon^M = \mathbf{B}^\varepsilon\mathbf{V}_1^\varepsilon\mathbf{m}_1^\varepsilon$, which can be done e.g. by the conjugate gradient technique described above for the overdetermined systems, used to minimise the residual

$$f_1(\mathbf{m_1}) := \left\|\varepsilon^M - \mathbf{B}^\varepsilon\mathbf{V}_1^\varepsilon\mathbf{m}_1\right\|^2. \tag{28}$$

  Since $\mathbf{B}^\varepsilon$ is already regularised, no Tikhonov regularisation term δ is necessary. Note that the regularisation of the system matrix perturbs its structure, hence instead of the optimised formulae (15), (16) and (19) their general counterparts have to be used.

3.2.3 Unreconstructible load component

Assume, given the noisy measurements ε^M and the relative accuracy $\varepsilon \geq 0$, that the corresponding regularised reconstructible load component $\mathbf{p}_R^\varepsilon$ has already been calculated. According to (25), any linear combination of columns of $\mathbf{V}_2^\varepsilon$ added to $\mathbf{p}_R^\varepsilon$ does not change the (noisy) system response ε^M. Therefore, all loads of the form

$$\mathbf{p} = \mathbf{p}_R^\varepsilon + \mathbf{V}_2^\varepsilon\mathbf{m}_2, \tag{29}$$

where $\mathbf{m}_2$ is a vector of arbitrary coefficients, are measurably indistinguishable and thus admissible regularised solutions to (12). The choice of a particular vector of coefficients $\mathbf{m}_2$ and the corresponding load $\mathbf{p}$ must be hence based on additional criteria, which are intrinsically heuristic and formulate *a priori* assumptions concerning anticipated characteristics of the load. These can be its non-negativity, norm-minimality, smoothness etc. The latter two can be obtained by choosing $\mathbf{m}_2$ such that the corresponding load (29) minimises the following objective function

$$f_2(\mathbf{m}_2) := \left\|\mathbf{D}\left(\mathbf{p}_R^\varepsilon + \mathbf{V}_2^\varepsilon\mathbf{m}_2\right)\right\|^2, \tag{30}$$

where $\mathbf{D}$ is an a priori given matrix (the identity, the first derivative $\mathbf{D}^1$ with respect to time and/or space etc.). Notice that:

1. Due to (24), $\mathbf{p}_R^\varepsilon$ is perpendicular to $span(\mathbf{V}_2^\varepsilon)$. Hence, if $\mathbf{D} = \mathbf{I}$, then $f_2(\mathbf{m}_2)$ is minimised by $\mathbf{m}_2 = \mathbf{0}$ and $\mathbf{p}_R^\varepsilon$ is the optimum load itself.

2. Since $f_2(\mathbf{m}_2)$ is a quadratic function, the f_2-optimum load depends linearly on $\mathbf{p}_R^\varepsilon$ and, due to (27), on the measurements ε^M:

$$\mathbf{p} = \left[\mathbf{I} - \mathbf{V}_2^\varepsilon \left(\mathbf{V}_2^{\varepsilon T}\mathbf{D}^T\mathbf{D}\,\mathbf{V}_2^\varepsilon\right)^{-1}\mathbf{V}_2^{\varepsilon T}\mathbf{D}^T\mathbf{D}\right]\mathbf{p}_R^\varepsilon. \tag{31}$$

A scrupulous analysis would reveal that in (29) and (30) upper bounds should be put on the moduli of the elements of $\mathbf{m}_2$ that corresponds to the columns of $\mathbf{V}_2^\varepsilon$ not belonging to $\mathbf{V}_2^0$. These columns represent the loads that do influence the measurement ε^M, although below the noise threshold ε.

3.2.4 Single-stage load identification

Instead of separate, successive identifications of the reconstructible and unreconstructible load components, the load can be identified in one stage only — however, at the cost of the accuracy. The objective functions $f_1(\mathbf{m}_1)$ of (28) and $f_2(\mathbf{m}_2)$ of (30) resemble the components of the general objective function $f(\mathbf{p})$, (14), which is used in the overdetermined case. Hence, instead of successive separate optimisations of $f_1(\mathbf{m}_1)$ and $f_2(\mathbf{m}_2)$, both functions may be optimised simultaneously, as in $f(\mathbf{p})$, weighted by an appropriate coefficient $\delta > 0$:

$$f_\delta(\mathbf{p}) := \left\|\varepsilon^M - \mathbf{B}\mathbf{p}\right\|^2 + \delta\left\|\mathbf{D}\mathbf{p}\right\|^2. \tag{32}$$

As the second term plays also the role of a regularisation term, there is no need to use the regularised system matrix $\mathbf{B}^\varepsilon$, and hence no need for numerically costly (although one-time only) singular value decomposition. The minimisation of the compound objective function f_δ can be performed relatively quickly by the conjugate gradient technique described earlier.

This one-stage approach makes no distinction between the reconstructible and the unreconstructible load components and retrieves them simultaneously. Therefore, it is generally less accurate, since the heuristic assumptions influence both components of the identified load, while the two-stage approach described in the preceding subsection properly identifies the reconstructible component on the basis of the measurements ε^M only.

3.3 Elasto-plastic systems

The approaches described before rely on the linearity of the system equation (12). The elasto-plastic case of (13) has to be treated separately. In general, three cases are possible:

1. *Strongly overdetermined* system, possible in the case of a very limited load area: The number of sensors exceeds or equals the total number of potentially load-exposed DOFs and potentially plastified truss elements. The approach described before for overdetermined linear systems is straightforwardly applicable with both loads $\mathbf{p}$ and plastic distortions β treated as independent unknowns.
2. *Overdetermined* system: The number of sensors exceeds or equals the number of potentially load-exposed DOFs. The unique evolution of the load can be identified, although the approaches of the preceding sections are not applicable, since the system is not linear.
3. *Underdetermined* system: Fewer sensors than potentially load-exposed DOFs. In general, the gradient-based optimisation approach presented below identifies a non-unique load, which is observationally indistinguishable from the actual load. Besides Tikhonov regularisation, other problem-specific regularising techniques can be used to additionally constrain the solution.

Notice that, even with sufficiently many sensors, a specific topology of the structure can make the system singular and effectively underdetermined.

In the overdetermined elasto-plastic case (13) can be, in general, uniquely solved by minimising the objective function (15) with any gradient-based optimisation algorithm. However, the modelled system response $\varepsilon(t)$ is no longer a linear function of the load $\mathbf{p}(t)$ and the derivatives instead of (16) take the following form:

$$\frac{\partial f(\mathbf{p})}{\partial p_n(t)} = \delta\frac{\partial\left\|\mathbf{D}\mathbf{p}\right\|^2}{\partial p_n(t)} - 2\sum_\alpha\sum_{\substack{\tau=\\ max(0,t)}}^{T}\left[\varepsilon_\alpha^M(\tau) - \varepsilon_\alpha(\tau)\right]\frac{\partial\varepsilon_\alpha(\tau)}{\partial p_n(t)}. \tag{33}$$

The first derivative is computable by (17), while the second, for $t \le \tau$, by (4) and (5), is

$$\frac{\partial\varepsilon_\alpha(\tau)}{\partial p_n(t)} = B_{\alpha n}(\tau - t) + \sum_{\kappa=t}^{\tau}\sum_\zeta B_{\alpha\zeta}^P(\tau-\kappa)\sum_{\nu=t}^{\kappa}\frac{\partial\Delta\beta_\zeta(\nu)}{\partial p_n(t)}.$$

The derivatives of the plastic flow $\Delta\beta_\zeta(\nu)$ with respect to the load $p_n(t)$ have to be computed prior to the derivatives of the objective function (33) by iteratively solving the following linear sets of equations, which are obtained by differentiating (10), and making use of (5) to compute the derivatives of the total plastic strain:

$$E_\alpha\sum_{\zeta\in Y_t}\left[B_{\alpha\zeta}^P(0) - \frac{\delta_{\alpha\zeta}}{1-\gamma_\alpha}\right]\frac{\partial\Delta\beta_\zeta(t)}{\partial p_n(t)} = -E_\alpha B_{\alpha n}(0),$$

$$E_\alpha\sum_{\zeta\in Y_{\nu+\Delta t}}\left[B_{\alpha\zeta}^P(0) - \frac{\delta_{\alpha\zeta}}{1-\gamma_\alpha}\right]\frac{\partial\Delta\beta_\zeta(\nu+\Delta t)}{\partial p_n(t)} = -\frac{\partial\sigma_\alpha^{\mathrm{tr}}(\nu+\Delta t)}{\partial p_n(t)} + \frac{\gamma_\alpha}{1-\gamma_\alpha}E_\alpha\sum_{\iota=t}^{\nu}\frac{\partial\Delta\beta_\alpha(\iota)}{\partial p_n(t)}\operatorname{sgn}\Delta\beta_\alpha(\iota)\operatorname{sgn}\sigma_\alpha^{\mathrm{tr}}(\nu+\Delta t),$$

where, by (7) and (4), the derivative of the trial stress is

$$\frac{\partial\sigma_\alpha^{\mathrm{tr}}(\nu+\Delta t)}{\partial p_n(t)} = E_\alpha B_{\alpha n}(\nu+\Delta t-t) + E_\alpha\sum_{\kappa=t}^{\nu+\Delta t}\sum_\zeta\left[B_{\alpha\zeta}^P(\nu+\Delta t-\kappa) - \delta_{\kappa\nu\alpha\zeta}\right]\sum_{\iota=t}^{\min(\kappa,\nu)}\frac{\partial\Delta\beta_\zeta(\iota)}{\partial p_n(t)},$$

where $\delta_{\kappa\nu\alpha\zeta}$ denotes Kronecker's delta.

4 Optimum sensor location and identification accuracy

In the load identification strategies described above crucial is the problem of accuracy. Due to masking by measurement noise and possible underdetermination, a part of the information about the load is completely lost in the measurement process and not retained in the measured data. The corresponding part of the load is unreconstructible: it can be assumed using some purely heuristic criteria, but there is no way to identify or estimate it from the measurement. Therefore, there are no specific (non-heuristic) *a posteriori* accuracy measures.

However, inaccuracy is associated with the unreconstructible load subspace, which directly depends on sensor location. It can be thus *a priori* minimised by a proper distribution of available sensors with respect to some optimality criteria. This seems to be a relatively unexplored problem. Mackiewicz et al (1996) study a related problem of static mode identification and propose to locate the sensors to ensure well-conditioning of the identification process and weak influence of interfering modes. Jacquelin et al (2005) study a single sensor single force reconstruction problem and observe a relation between its conditioning and certain characteristics of the frequency response function (alternate succession of resonances and antiresonances), which in multi-sensor and multi-force cases can be potentially used to designate a finite and limited-size set of candidate sensor locations to choose from based on other more specific optimality criteria. This section introduces two such estimates of reconstruction accuracy, which are based either on the dimension of the unreconstructible load subspace (via a correlated feature of conditioning) or on its coincidence with a given set of expected or typical loads. Since these criteria tend to be negatively correlated, a third, compound criterion is proposed, which can be thus seen as a single *a priori* measure of reconstruction accuracy. However, only linear systems are considered. The problem of optimum sensor location in case of elasto-plastic systems requires further study.

A sensor location is denoted by π and can be represented by a non-empty subset of $\{1,2,\ldots,A_{max}\}$, where A_{max} is the number of all possible locations of a single sensor throughout the structure.

4.1 Conditioning

The conditioning criterion is formalised here as the task of finding the sensor location π, which minimises the following measure of ill-conditioning of the corresponding system matrix $\mathbf{B}_\pi$

$$q_1(\pi) = \log \frac{\sigma_{max}(\mathbf{B}_\pi)}{\sigma_{median}(\mathbf{B}_\pi)}, \tag{34}$$

where $\sigma_{max}(\mathbf{B}_\pi)$ and $\sigma_{median}(\mathbf{B}_\pi)$ are the maximum and the median singular values of $\mathbf{B}_\pi$.

Note that the matrix condition number, which is the standard measure of conditioning of a matrix, involves the *minimum* singular value instead of the *median* used in (34). However, with inaccurate floating-point computer arithmetic the median is more reliable, since for strongly ill-conditioned matrices the calculated minimum singular value usually lies at a predefined cut-off level, defined by the accuracy of the arithmetic used.

4.2 Utility

In underdetermined systems along the ill-conditioning and nonuniqueness of solution arises also a related problem of the accuracy of identification. The identification process may be very well-conditioned, but it is of no use, if identified loads differ much from actual loads. For a given load the accuracy of identification can be quantified as a distance between the load and its reconstructible component.

Therefore, since actual loads are unknown, the utility of sensor location can be defined with respect to a given set of (expected or typical) unit loads $\{\mathbf{p}_1,\mathbf{p}_1,\ldots,\mathbf{p}_M\}$ as the mean square distance between the loads and their reconstructible components, see (26):

$$q_2(\pi) = \frac{1}{M}\sum_{i=1}^{M} \left\| \left(\mathbf{I} - \mathbf{V}_{1\pi}\mathbf{V}_{1\pi}^T\right)\mathbf{p}_i \right\|^2 = \frac{1}{M}\sum_{i=1}^{M} \left\| \mathbf{V}_{2\pi}\mathbf{V}_{2\pi}^T\mathbf{p}_i \right\|^2, \tag{35}$$

where $\mathbf{V}_{1\pi}$ and $\mathbf{V}_{2\pi}$ denote the matrices $\mathbf{V}_1$ and $\mathbf{V}_2$ calculated for a given sensor location π. Note that practical usefulness of q_2 depends on the set of unit loads $\{\mathbf{p}_1,\ldots,\mathbf{p}_M\}$, which should be well-suited to the loads expected in the investigated system.

4.3 Compound criterion

The conditioning and the utility criteria tend to be negatively correlated, see the numerical example in Figure 2. Moreover, criterion q_2 assumes no measurement noise, which can significantly diminish the accuracy of identification. Therefore, for practical reasons the ultimate criterion has to weight accuracy against conditioning, taking into account the relative measurement noise level ε. This can be achieved by measuring the accuracy of the identification process performed with the regularised system matrix $\mathbf{B}^\varepsilon$ instead of the original matrix $\mathbf{B}$:

$$q_2^\varepsilon(\pi) = \frac{1}{M}\sum_{i=1}^{M} \left\| \mathbf{V}_{2\pi}^\varepsilon \mathbf{V}_{2\pi}^{\varepsilon\,T}\mathbf{p}_i \right\|^2. \tag{36}$$

5 Numerical example

5.1 Structure

Figure 1 shows the modelled truss structure. It is 6 m long, the elements are 10 mm^2 in cross-section, 0.5 m or $0.5\sqrt{2}$ m

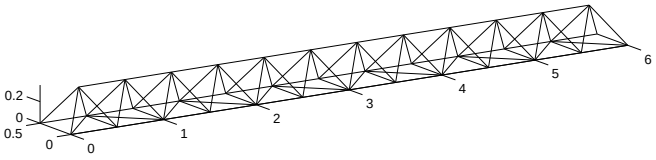

Fig. 1 Truss structure modelled in the numerical example

long, and made of steel with density 7800 kg/m^3, Young's modulus 200 GPa and — used in the elasto-plastic case only — initial plastic flow stress 50 MPa with hardening coefficient 0.01. The two left hand side corner nodes of the bottom plane were deprived of all degrees of freedom, while the two opposite right hand side corner nodes were deprived of the vertical degree of freedom and are free to move in the horizontal plane only.

Loading forces can occur only vertically in any/all of the 12 upper nodes of the structure. This assumption allows to depict evolution of loads in time-space in the convenient and illustrative form of a 2D graph. The *measurement* time interval is $T = 10$ ms, and has been discretised into 100 time steps of $\Delta t = 0.1$ ms each. The time shift is $\Delta T = 1$ ms, and hence the *reconstruction* time interval is $T + \Delta T = 11$ ms long (110 time steps). A total of A strain sensors, $A \in \{1,2,\ldots,11\}$, can be located in any of the eleven upper elements, which join the twelve potentially load-exposed nodes. The system transfer matrix $\mathbf{B}$ is hence $100A \times 1320$ and thus underdetermined. It has been generated using the Newmark integration scheme.

5.2 Sensor locations

For each of 2047 possible sensor locations π (non-empty subsets of the eleven strain sensors), both sensor location criteria q_1 and q_2, defined by (34) and (35), have been computed. Figure 2 plots q_2 versus q_1 to illustrate the negative correlation; each dot corresponds to one sensor location π. A clear arrangement in groups corresponding to the number of sensors A can be seen: the more sensors, the worse (larger) is the conditioning q_1 and the better (smaller) the accuracy q_2. Within the individual groups a slight positive correlation can be observed, although this is not always the case (Jankowski et al 2007).

The criterion q_2 has been calculated with respect to an arbitrary set of 144 simple impact unit loads $\mathbf{p}_i$. Each unit load acts 1.9 ms (19 time steps) in three neighbouring load-exposed DOFs, see Figure 3. This simple load pattern has been replicated and on a regular grid basis uniformly distributed in time and space (over the considered 110 ms interval and the 12 potentially load-exposed DOFs) to form all of the unit loads $\mathbf{p}_i$.

A measurement noise level of 5% rms has been assumed. Table 2 lists the best and the worst locations of three, four and five sensors computed with respect to the compound criterion $q_2^{5\%}$, (36). The best locations seem to distribute the sensors evenly, while the worst locations group the sensors together near the supports. In a comparable result obtained for a cantilever beam, the worst locations were grouped near the free end of the beam, while the more evenly distributed best locations preferred the fixed end (Jankowski et al 2007).

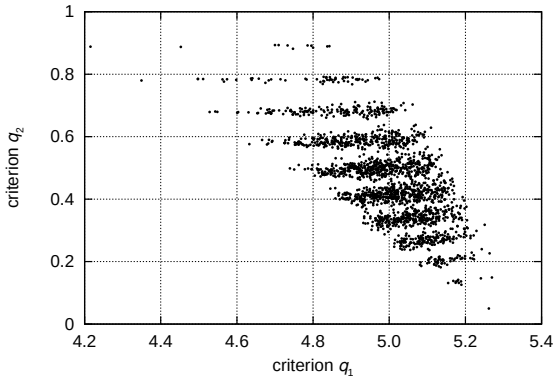

Fig. 2 Correlation plot for sensor location criteria q_1 and q_2

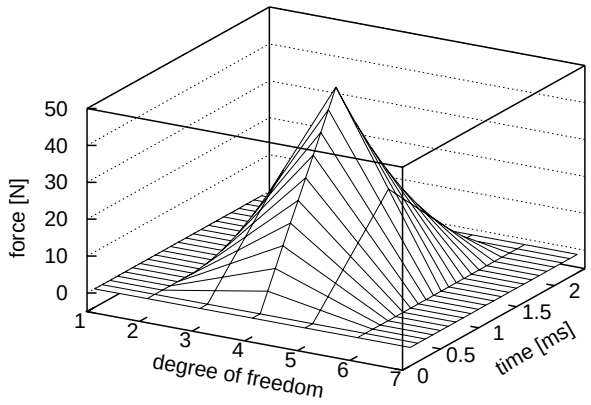

Fig. 3 Load pattern replicated 144 times and distributed in time and space to form all unit loads used for calculating criterion q_2

Table 2 Five best and worst locations of three, four and five sensors with respect to $q_2^{5\%}$ (each "o" denotes one sensor)

	three sensors	four sensors	five sensors
$q_2^{5\%}$-best	-o-o-----o-	-o-o-o---o-	oo---o-o--o
	-o-o------o	-o-o---o-o-	o--o-o---oo
	-o---o---o-	-o-o-o----o	-o-o--o--oo
	-o-----o-o-	-o-o-----oo	oo--o-o--o-
	-o--o----o-	-o-o----o-o	-o--o-o--oo
$q_2^{5\%}$-worst	--------ooo	-------oooo	------ooooo
	ooo--------	oooo-------	ooooo------
	-ooo-------	------oooo-	-----ooooo-
	------ooo--	-----oooo--	----ooooo--
	-----ooo---	-oooo------	-----o-oooo

5.3 Actual load

Figure 4 depicts the evolution of the assumed actual load, which is to be identified in the following with the discussed approaches. The load occurs vertically in the vicinity of the fourth upper level node and starts moving towards right.

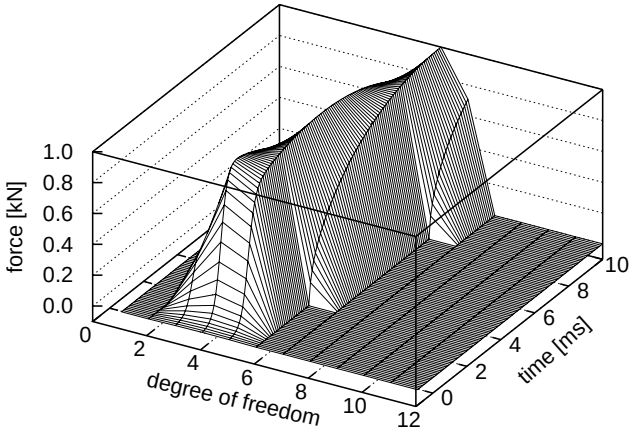

Fig. 4 Assumed actual load (vertical forces in 12 upper level nodes)

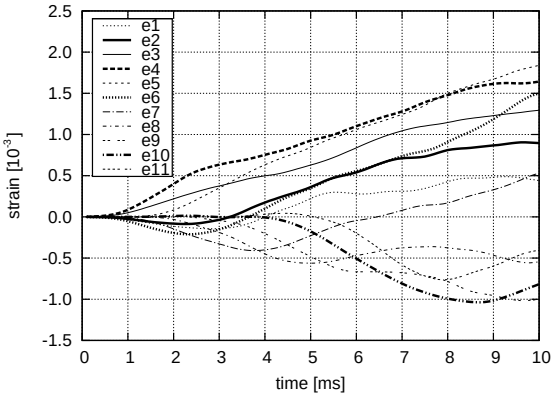

Fig. 5 Elastic case, computed exact responses of eleven considered strain sensors (upper elements 1 to 11)

5.4 Elastic case

Figure 5 plots the computed exact responses of all eleven considered sensors. The bold lines mark the responses of the four $q_2^{5\%}$-best located sensors (no. 2, 4, 6 and 10), which have been used for reconstruction. Figure 6 illustrates the structure of the corresponding system transfer matrix $\mathbf{B}$: row blocks correspond to the four sensors, column blocks to the eleven potentially load-exposed degrees of freedom and since there are 100 reconstruction and 110 loading time steps, each block is a 100×110 Toeplitz matrix. Figure 7 plots the first 150 singular values of the matrix across the orders of magnitude and compares them with the singular values computed for the $q_2^{5\%}$-worst location. Even in the $q_2^{5\%}$-best case only the first 87 singular vectors stay above the 5% noise limit, become the matrix $\mathbf{V}_1^{5\%}$ and represent loads constituting an orthonormal basis in the space of the reconstructible loads. Examples are shown in Figure 8. Notice the increasing oscillations: the consecutive singular vectors introduce more and more high frequency components. The unreconstructible subspace $V_2^{5\%}$ of noise-sensitive loads is thus spanned only by high frequency loads, and the reconstructible load $\mathbf{p}_R^{5\%}$ is generally of lower (time-space) frequency than the actual load $\mathbf{p}$, since the high frequency unreconstructible components are cut off in the regularisation process.

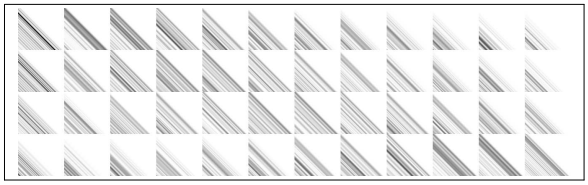

Fig. 6 Elastic case, $q_2^{5\%}$-best location of four sensors: structure of system transfer matrix

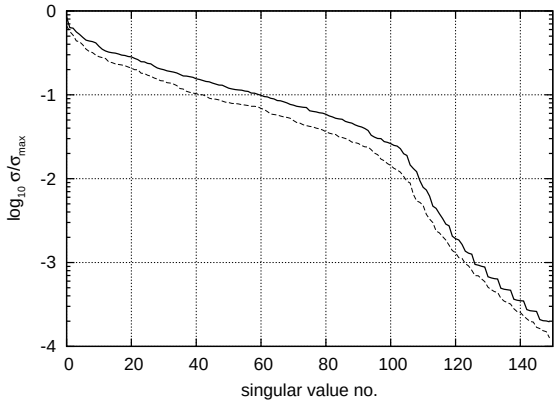

Fig. 7 Elastic case, first 150 singular values of system transfer matrix plotted across orders of magnitude, $q_2^{5\%}$-best (continuous) and $q_2^{5\%}$-worst (dashed) locations of four sensors

The responses of the four $q_2^{5\%}$-best sensors have been contaminated with numerically generated Gaussian noise at the 5% rms level and used to obtain by (27) the reconstructible component $\mathbf{p}_R^{5\%}$, which is shown in Figure 9 (top left). Full heuristic identification has been performed by (31) with the heuristic assumption weighting smoothness w.r.t time against smoothness w.r.t. space (degrees of freedom) by

$$\mathbf{D} = \begin{bmatrix} (1-\mu)\,\mathbf{D}_{\text{time}}^{1} \\ \mu\,\mathbf{D}_{\text{dof}}^{1} \end{bmatrix}. \tag{37}$$

Figure 9 (top right) plots the result computed for $\mu = 0.38$ (the value found with the L-curve method), while the two bottom figures illustrate the sensitivity of the results to the weighting parameter μ. For comparison, Figure 10 shows the results of the single-stage load reconstruction by (32) with the weighting parameter δ determined by the L-curve method (left figure) and the reconstructible component computed at the $q_2^{5\%}$-worst sensor location $\{8, 9, 10, 11\}$ (right figure).

5.5 Elasto-plastic case

In the elasto-plastic case the actual load plastifies 17 elements out of the total of 107, including seven elements potentially equipped with strain sensors (upper elements no. 4 to 10). Figure 11 (top left) plots the computed exact strains

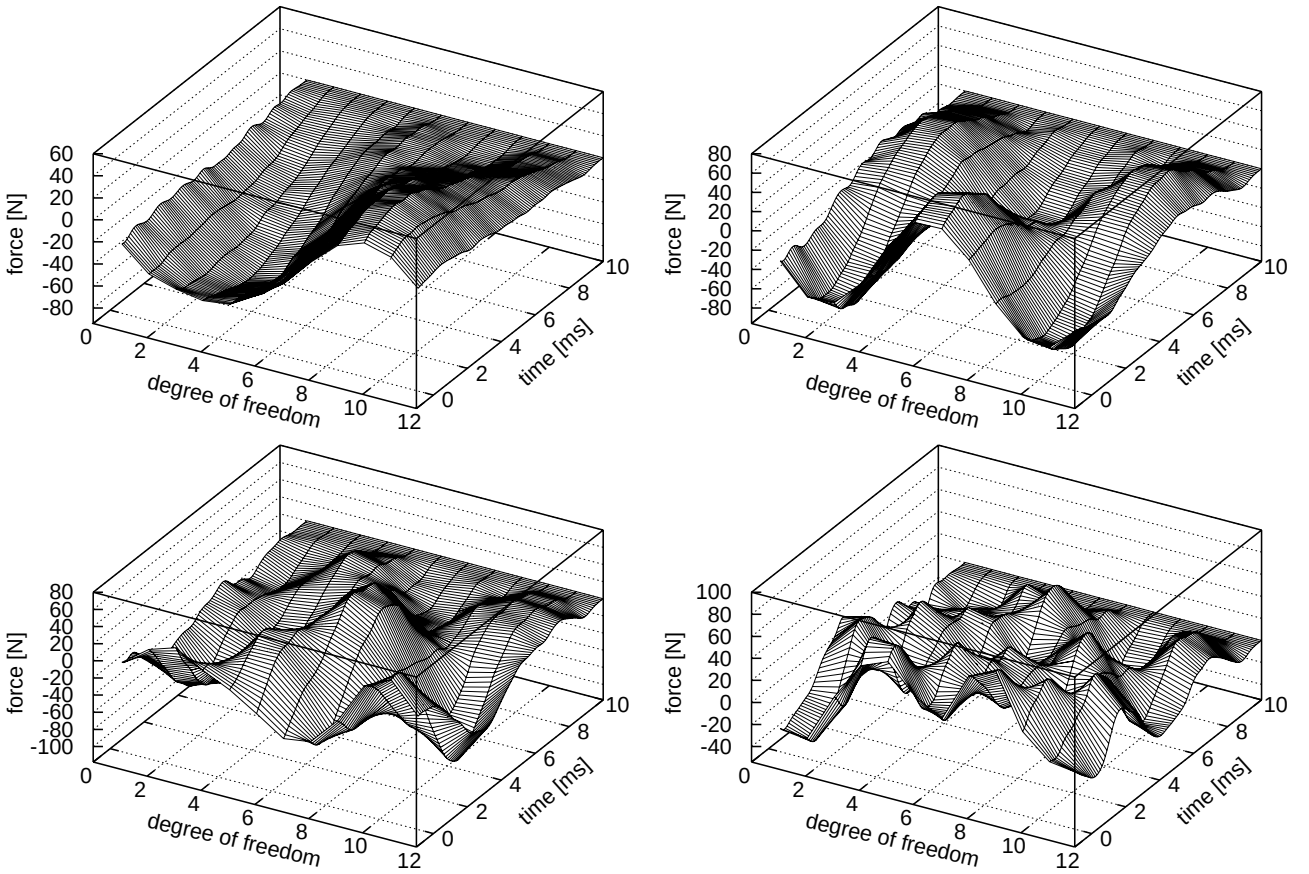

Fig. 8 Elastic case, loads corresponding to 1^{st} to 3^{rd} and 6^{th} (top left to bottom right) singular vectors computed for $q_2^{5\%}$-best location of four sensors

of all eleven upper elements, the differences to the purely elastic case (Figure 5) are clearly visible.

A load, which is observationally indistinguishable from the actual load, can be found by solving (13). This equation is non-linear with respect to the load, hence the decomposition and regularisation technique of the elastic system cannot be used. Therefore, the residuum of (13) has been minimised with the gradient-based approach described above and the Levenberg-Marquardt optimisation method with the zero load as the starting point. Since the considered case is underdetermined, the solution is non-unique and has been additionally constrained by requiring its non-negativity. The objective function (15) implemented the non-negativity requirement by using an exterior quadratic penalty function instead of the Tikhonov regularisation term.

The result of the identification with the $q_2^{5\%}$-best location of four sensors is shown in Figure 11 (top right), 5% rms Gaussian noise has been used. The effect of the noise is illustrated by the figures in the bottom line, which show the results of the identification with and without the noise at the $q_2^{5\%}$-best location of five sensors. The bottom right figure confirms also the existence of local minima of the objective function: the identified load is a local minimum only, since the global minimum is defined by the actual load, Figure 4.

6 Conclusions

This paper describes a methodology for impact load identification in elastic and elasto-plastic structures. It aims at reliable identification of general loads, including moving and simultaneous multiple load cases, with a limited number of sensors. The identification is based on optimisation of local responses, in the elastic case makes use of the decomposition of the load into reconstructible and unreconstructible components, and can be stored in a black-box system for a posteriori reconstruction of accident scenario.

The research is ongoing to limit the considerable numerical effort required for identification and further investigate the problem of optimum sensor location. Efficiency of related numerical algorithms for load identification in case of elasto-plastic structures is a subject of an upcoming paper.

References

Adams R, Doyle JF (2002) Multiple force identification for complex structures. Experimental Mechanics 42(1):25–36

Chan THT, Yu L, Law SS (2001) Moving force identification studies: Theory. Journal of Sound and Vibration 247(1):59–76

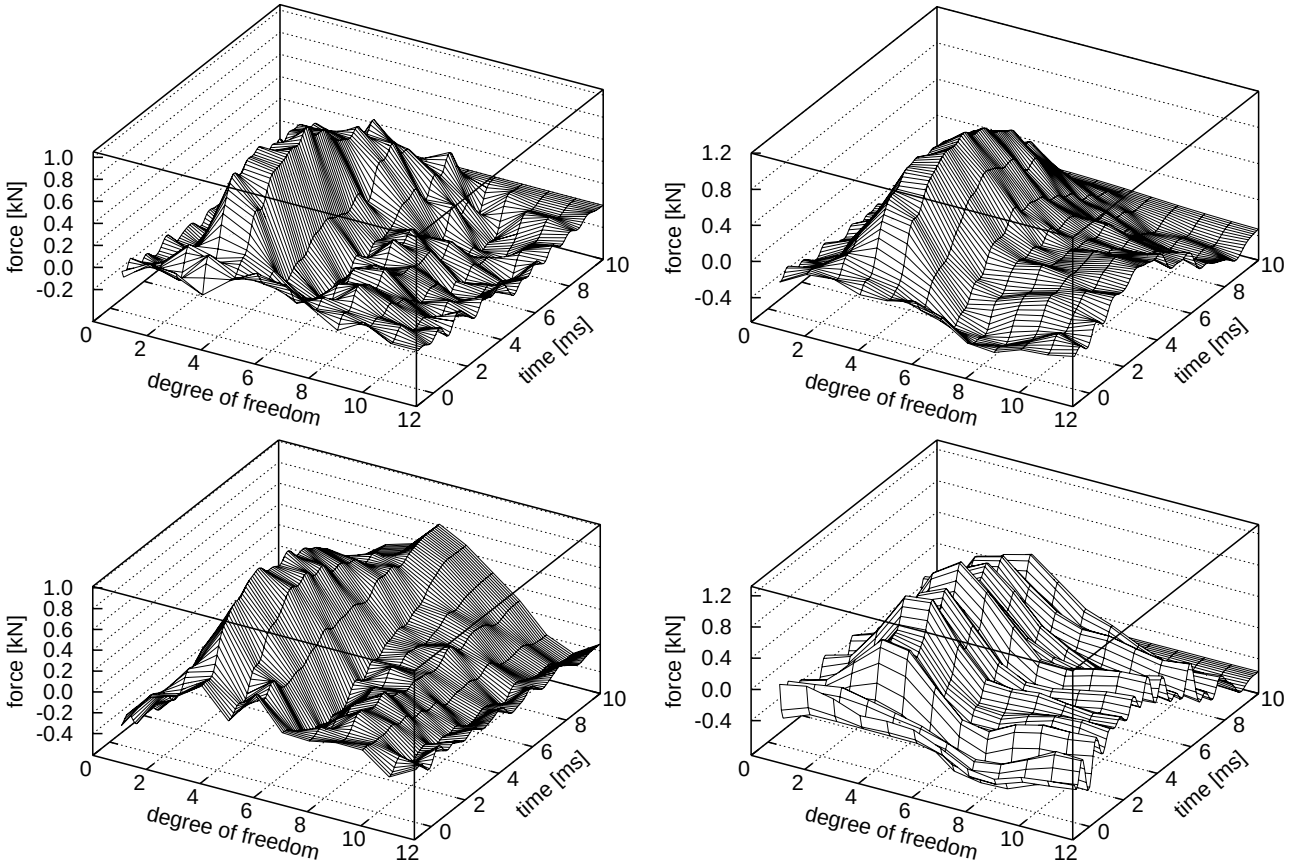

Fig. 9 Elastic case, numerical example of load identification computed for the $q_2^{5\%}$-best location of four sensors at noise level 5% rms: (top left) reconstructible load component $\mathbf{p}_R^{5\%}$; (top right) heuristic identification by (31) and (37) with $\mu = 0.38$; (bottom left) heuristic identification with $\mu = 0.01$; (bottom right) heuristic identification with $\mu = 0.9$

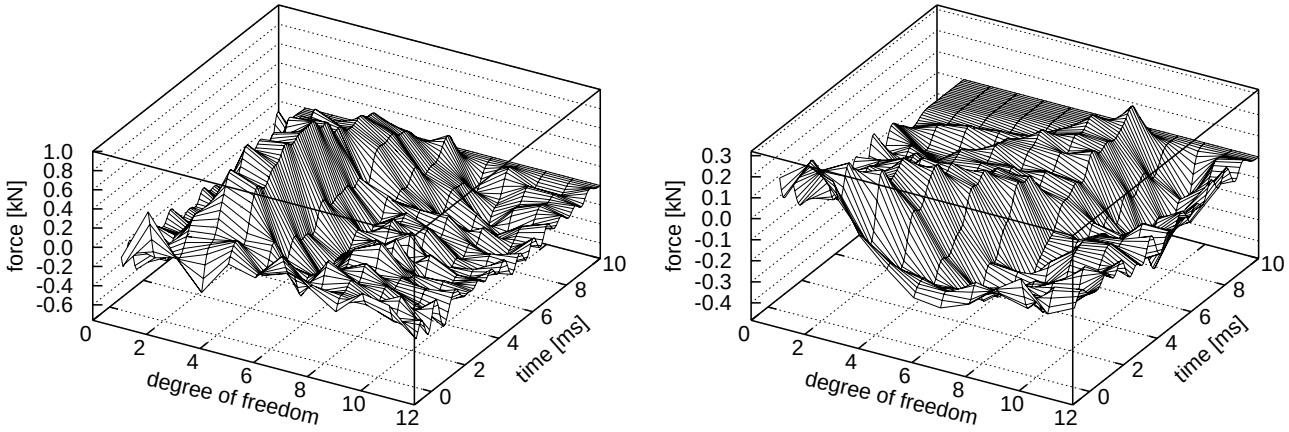

Fig. 10 Elastic case, numerical example of load identification: (left) single-stage load reconstruction computed at $q_2^{5\%}$-best location of four sensors; (right) reconstructible component computed at $q_2^{5\%}$-worst location of four sensors

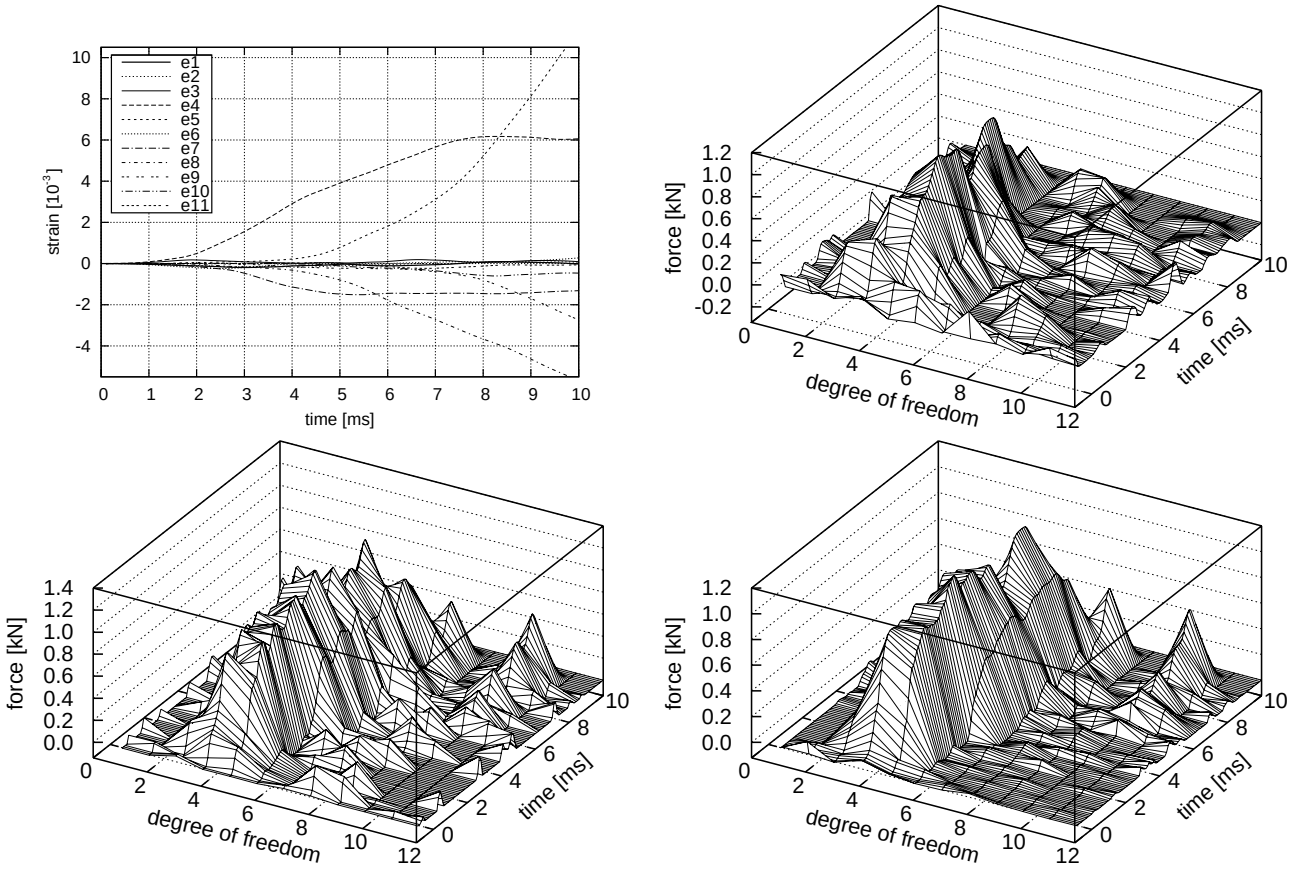

Fig. 11 Elasto-plastic case, numerical example of load identification: (top left) computed exact responses of eleven considered strain sensors (upper elements 1 to 11); (top right) load identified at 5% rms noise level with $q_2^{5\%}$-best location of four sensors; (bottom left) load identified at 5% rms noise level with $q_2^{5\%}$-best location of five sensors; (bottom right) load identified without noise contamination with $q_2^{5\%}$-best location of five sensors

Dahlquist G, Bjørck A (2006) Numerical Methods in Scientific Computing. to be published by SIAM, Philadelphia

Fukunaga H, Hu N (2006) Experimental impact force identification of composite structures. In: Proc. of 3rd European Workshop on Structural Health Monitoring, pp 840–847

Gaul L, Hurlebaus S (1997) Identification of the impact location on a plate using wavelets. Mechanical Systems and System Processing 12(6):783–795

Hansen P (2002) Deconvolution and regularization with toeplitz matrices. Numerical Algorithms 29:323–378

Holnicki-Szulc J, Gierliński J (1995) Structural Analysis, Design and Control by the Virtual Distortion Method. Wiley, Chichester

Inoue H, Harrigan J, Reid S (2001) Review of inverse analysis for indirect measurement of impact force. Applied Mechanics Reviews 54(6):503–524

Jacquelin E, Bennani A, Hamelin P (2003) Force reconstruction: analysis and regularization of a deconvolution problem. Journal of Sound and Vibration 265:81–107

Jacquelin E, Bennani A, Massenzio M (2005) Analysis of a force reconstruction problem. Structural Engineering and Mechanics 21(3):237–254

Jankowski L, Wikło M, Holnicki-Szulc J (2007) Robust post-accident reconstruction of loading forces. Key Engineering Materials 347:659–664

Kress R (1989) Linear integral equations, Applied Mathematical Sciences, vol 82. Springer, New York

Law SS, Chan THT, Zeng QH (1997) Moving force identification: A time domain method. Journal of Sound and Vibration 201(1):1–22

Mackiewicz A, Holnicki-Szulc J, Lopez-Almansa F (1996) Optimal sensor location in active control of flexible structures. AIAA Journal 34(4):857–859

Martin MT, Doyle JF (1996) Impact force location in frame structures. International Journal of Impact Engineering 18(1):79–97

Nocedal J, Wright S (1999) Numerical Optimization. Springer Series in Operations Research, Springer, New York

Putresza JT, Kołakowski P (2001) Sensitivity analysis of frame structures — Virtual Distortion Method approach. International Journal for Numerical Methods in Engineering 50(6):1307–1329

Simo JC, Hughes TJR (1989) Computational inelasticity, Interdisciplinary Applied Mathematics, vol 7. Springer

Tikhonov A, Arsenin V (1977) Solutions of Ill-posed Problems. Wiley, New York

Wikło M, Holnicki-Szulc J (2008) Optimal design of adaptive structures. Part II: Adaptation to impact loads. Structural and Multidisciplinary Optimization, in press

Wu E, Tsai CZ, Tseng LH (1998) A deconvolution method for force reconstruction in rods under axial impact. Journal of Acoustical Society of America 104(3):1418–1426